

# Shear-driven solidification of dilute colloidal suspensions

Alessio Zaccone<sup>1</sup>, Daniele Gentili<sup>1</sup>, Hua Wu<sup>1</sup>, Massimo Morbidelli<sup>1</sup>, and Emanuela Del Gado<sup>2</sup>

<sup>1</sup>Chemistry and Applied Biosciences, ETH Zürich, CH-8093 Zürich, Switzerland and

<sup>2</sup>Microstructure and Rheology, Institute for Building Materials, ETH Zürich, CH-8093 Zürich, Switzerland

(Dated: May 29, 2022)

We show that the shear-induced solidification of dilute charge-stabilized (DLVO) colloids is due to the interplay between the shear-induced formation and breakage of large non-Brownian clusters. While their size is limited by breakage, their number density increases with the shearing-time. Upon flow cessation, the dense packing of clusters interconnects into a rigid state by means of *grainy* bonds, each involving a large number of primary colloidal bonds. The emerging picture of shear-driven solidification in dilute colloidal suspensions combines the gelation of Brownian systems with the jamming of athermal systems.

PACS numbers: 82.70.Dd, 83.60.Rs, 64.70.pv

Shear-driven solidification of diluted colloidal suspensions has dramatic impact on their applications, from industrial polymer production to natural microfluidic devices [1, 2], and is a prototype of non-equilibrium transitions. If interparticle interactions are purely attractive, the applied shear stress may break down aggregates and fluidize the material [3, 4]. However, the colloidal particles are often stabilized by electrostatics [1], with no tendency to aggregate at rest, and high shear rates may ultimately promote aggregation in competition with the electrostatics. The interplay between these two tendencies may lead to persistent structures [5] and this shear-induced aggregation might be as dramatic as a complete solidification of even diluted suspensions, hence seriously affecting the material and rheological properties. Although this is a widely reported phenomenon in both artificial and living systems [2, 5, 6], there is little understanding of the solidification mechanism. This is due to the difficulty to monitor the system with real-space optics or scattering techniques at high shear rates [5, 6]. To overcome these obstacles, we have designed an experimental protocol exploiting charge-stabilized colloidal particles which interact via a typical DLVO potential [1] where an energy barrier coexists with a deep, shorter-ranged attractive well. In our setup, shear-induced aggregation can be monitored in a fully controlled way, allowing for the first time to rationalize the effect of the shear stress from an initially dilute suspension to the final solid. By combining light scattering, rheology, and microscopy data we formulate a model for the solidification mechanism. The effective packing fraction of the aggregates formed under shear increases with time. Upon flow cessation their dense packing is progressively frozen into a rigid structure by the formation of *grainy* (i.e., multiple) colloidal bonds which are responsible for the fairly high shear moduli observed.

*Experiments.* The system consists of colloidal particles at a fixed colloid volume fraction of  $\phi \simeq 0.21$ . For the effective DLVO interaction [1], the attractive well depth is  $\simeq 40k_B T$  and the repulsive barrier  $\simeq 60k_B T$ . The col-

loidal particles are surfactant-free polystyrene-acrylate latex spheres charge-stabilized by the charged groups of the initiator [2]. The nearly monodisperse particles have mean radius  $a \simeq 60nm$  as determined from both dynamic and static light scattering (using a BI-200 SM goniometer system, Brookhaven Instruments, NY).  $17mM$  of NaCl were added to weakly screen the electrostatic interaction barrier, characterized by Zeta-potential measurements. A strain-controlled ARES rheometer (Advanced Rheometric Expansion System, TA Instruments, Germany) with Couette geometry has been employed to induce the shear flow under shear-rate control and to measure the rheological properties. We have initially sheared the system for a varying time  $\tau_1$  at a fixed shear-rate ( $1700s^{-1}$ ). For each  $\tau_1$ , upon flow cessation, we sampled the shear cell and analyzed the system by laser light scattering (LLS) using a small-angle light scattering Mastersizer 2000 instrument (Malvern, U.K). The LLS analysis can be done off-line since the aggregation does not evolve on the time scale of the analysis in the absence of shear. The samples were diluted at  $\dot{\gamma} = 0$  to such an extent that multiple light scattering does not affect the measurement. After each  $\tau_1$  we have also performed rheological shear-sweep and frequency-sweep tests. Since the height of the energy barrier for bond-breaking is  $\sim 100k_B T$ , the clusters are mechanically stable even under the fairly high shear rate of the Couette cell, hence it is clear that they cannot de-aggregate during the off-line analysis. From the scattered intensity  $I(q)$  we obtain the average structure factor of the aggregates  $\langle S(q) \rangle$  [3] (not to be confused with the one of the whole suspension) present in the system at the time of sampling.

*Results and discussion.* The starting point of our analysis is the time evolution of the systems sheared at a constant shear rate  $\dot{\gamma} = 1700s^{-1}$ . The viscosity shows a sharp upturn in time, after an induction delay due to the activation barrier in the microscopic aggregation kinetics between two colloidal particles [1]. The barrier for shear-induced aggregation, in fact, decreases exponentially upon increasing the shear rate and vanishes upon

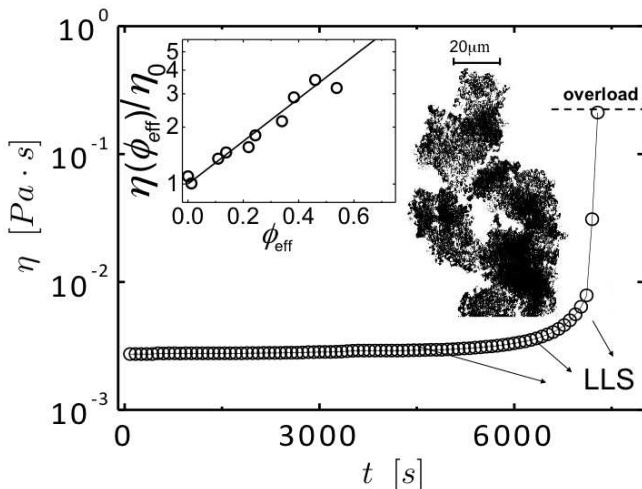


FIG. 1. Main frame: Time evolution of the viscosity  $\eta$  at  $\dot{\gamma} = 1700s^{-1}$  and  $\phi \simeq 0.21$ . Insets: left -  $\eta/\eta_0$  as a function of  $\phi_{eff}$  from experiments (circles) and the extended Einstein formula (line); right - Optical micrograph upon flow cessation.

reaching a certain cluster size above which the aggregation kinetics is much faster and goes with the cube of the cluster size [1]. Hence a kind of self-accelerated kinetics, leading to larger and larger aggregates, is expected once clusters of a critical size are formed. On the other hand, the action of shear is also well known to cause fragmentation, which should ultimately lead to a maximal cluster size, dictated by the mechanical balance between the stress imposed by the flow on the cluster and its mechanical response. Nevertheless we observe (Fig.1, main frame) that the viscosity continues to increase until the instrument stress overload threshold is reached. We have stopped the shearing after different time duration  $\tau_1$  (*pre-shearing* times). For each  $\tau_1$  we have used optical microscopy and LLS to investigate the structure of the resulting suspension. An optical micrograph upon flow cessation at the largest  $\tau_1$  is shown in the inset (right) of Fig.1. From the small angle light scattering analysis [10], it is evident that already after a short time the size distribution of aggregates is strongly bimodal (i.e., primary particles coexist with large aggregates). The Guinier plot gives a typical aggregate radius, resulting from the competition between aggregation and breakage,  $R_g \simeq 35 \pm 3 \mu m$  which remains constant with time [10], indicating that the aggregation under shear rapidly leads to an optimal cluster size. From the power-law regime of the scattering curves we extract the fractal dimension  $d_f$  of the large clusters: as a function of  $\tau_1$  [10]  $d_f$  also rapidly reaches a plateau at  $\simeq 2.7 \pm 0.1$ , a fairly high value which is typical of shear-driven aggregation [6] where breakage events and restructuring induced by flow stresses combine [7]. We have measured the fraction  $\chi(t)$  of primary colloidal particles converted to clusters and found that it steeply increases [10]. The emerging picture is that under shear the system is constantly generating new clusters

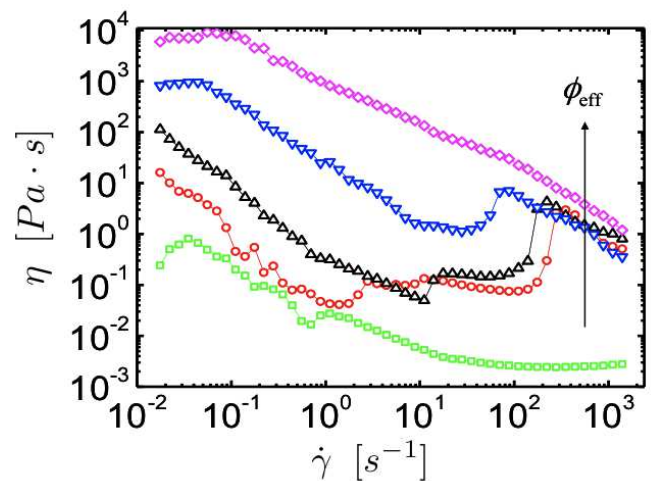


FIG. 2. (color online) Shear-sweep curves obtained after pre-shearing at  $\dot{\gamma} = 1700s^{-1}$  for  $\tau_1 = 4054s, 7420s, 7500s, 7520s$  and  $7555s$  (from bottom to top).

with approximately the same size  $R_g$  and fractal dimension  $d_f$ . The fast increase in the number density of clusters which are fractal and porous is associated with a rapid increase of their effective packing fraction: this could be the reason for the sharp non-linear increase of the viscosity in Fig.1. To test this hypothesis, we have estimated the clusters effective packing fraction  $\phi_{eff}$  through the relation  $\phi_{eff}(t) = \chi(t)\phi k^{-1}(R_g/a)^{3-d_f}$ , where  $k$  is a geometric prefactor close to one and  $\phi$  is the initial volume fraction of primary particles [5]. In the inset (left) of Fig.1 we plot the viscosity  $\eta(t)$  (circles), normalized by  $\eta_0$ , as a function of  $\phi_{eff}(t)$ . We have also calculated the high shear viscosity of an equivalent suspension of hard spheres of the same linear size at the same volume fraction  $\phi_{eff}(t)$ , using the Einstein formula properly extended to high  $\phi_{eff}(t)$  [15] which gives  $\eta \simeq \eta_0 \exp(5\phi_{eff}(t)/2)$  (the full line in the same inset). The agreement indicates that the increase of the viscosity under shear in Fig.1 can be ascribed indeed to the increasing packing fraction of the clusters, which hydrodynamically behave as hard spheres due to the fairly high  $d_f$  [16]: the initial dilute colloidal suspension has changed, under shear, into a suspension of non-Brownian aggregates whose packing fraction increases with the shearing time.

After each of the pre-shearing times, we also perform a shear-sweep experiment where  $\dot{\gamma}$  is varied but kept below  $\dot{\gamma} = 1700s^{-1}$ . This guarantees that the aggregates formed during the pre-shearing are mechanically stable and do not break up during the shear-sweep [17, 18]. The data are plotted in Fig.2. The curves correspond to  $\tau_1 = 4054s, 7420s, 7500s, 7520s$  and  $7555s$  from bottom to top, and to  $\phi_{eff}(\tau_1)$  increasing accordingly. For the shortest  $\tau_1$ , a modest shear-thinning is followed by a Newtonian plateau. Upon increasing  $\tau_1$ , the viscosity curves are shifted to higher values and a steep shear-

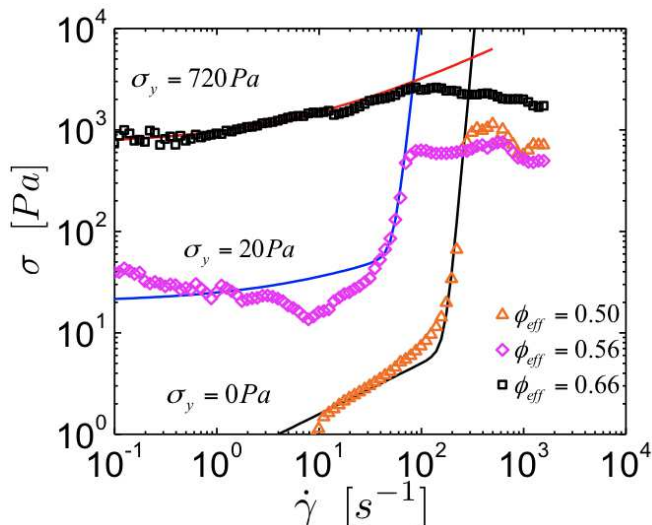


FIG. 3. (color online) The measured stress as a function of shear rate (symbols) and the extended Herschel-Bulkley curves (lines) [26].

thickening appears: the rheological behavior of our system upon increasing  $\tau_1$  is qualitatively the same as the one of dense non-Brownian suspensions upon increasing volume fraction [19, 20]. Note that flow inhomogeneity may occur in this type of measurements [21, 22] and we cannot exclude its presence here (although MRI studies in a very similar system [23] detected shear banding only for  $\dot{\gamma} < 60 s^{-1}$ ). Thus Fig.2 gives only macroscopic rheological information, possibly dependent on the geometry. A shear thinning followed by a shear thickening regime has also been observed in some gelling colloidal suspensions [24], where it has been explained in terms of an increase of the clusters number density due to break-up. Here we have made sure that the shear-sweep is done at  $\dot{\gamma}$  lower than the value needed for breaking up the clusters, therefore we rather associate the shear thickening to the formation of inter-clusters bonds, possibly also promoted by hydrodynamic interactions [25] and/or from a residual inter-cluster attraction: the shear rate is too low to break the pre-formed aggregates but can promote, instead, the formation of further bonds among them. At the largest  $\phi_{eff}$  (i.e.,  $\tau_1$ ) the shear-thickening is no longer visible. The behavior of the stress intensity  $\sigma$  as a function of  $\dot{\gamma}$  plotted in Fig.3 sheds some light on this rheological behavior. For large  $\phi_{eff}$  the curves can be well described with an extended Herschel-Bulkley type of behavior, which accounts for shear-thickening [26],  $\sigma(\dot{\gamma}) = \sigma_y + a_1 \dot{\gamma}^{1/2} + a_2 \dot{\gamma}^{1/\epsilon}$  where  $\sigma_y$  is the yield stress,  $a_1$  and  $a_2$  are parameters depending on  $\phi_{eff}$  and  $\epsilon < 0.1$  is typically obtained for the steep shear thickening of densely packed non-Brownian suspensions [26]. This indicates that the onset of the yield stress occurs in the range of effective volume fractions  $0.50 < \phi_{eff} < 0.56$ . At  $\phi_{eff} \simeq 0.66$ , i.e. the largest value obtained here, the yield stress has now a value close to the upper stress

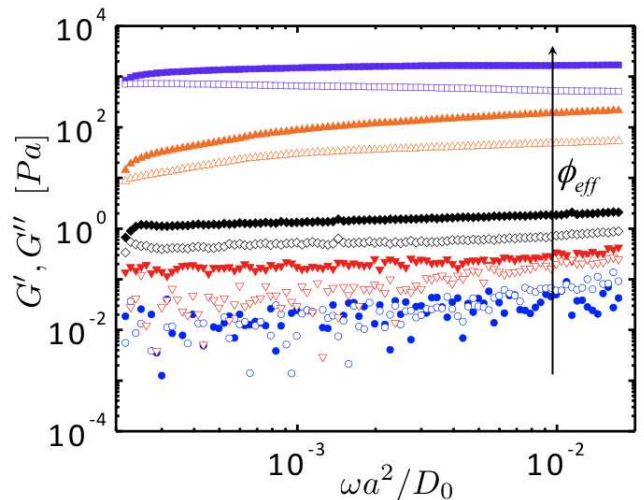


FIG. 4. (color online)  $G'$  (filled symbols) and  $G''$  (open symbols) measured after  $\tau_1 = 4054s, 6350s, 7400s$  and  $7480s$  (from bottom to top) as a function of the frequency  $\omega$  in units of the diffusion time in the dilute limit,  $\tau_0 = a^2/D_0$ .

limit of the shear thickening and this makes the shear thickening no longer visible. The same phenomenon has been observed indeed in densely packed non-Brownian suspensions. Hence, in a dilute colloidal system at a solid fraction  $\phi = 0.21$  we get the whole rich phenomenology observed in non-Brownian suspensions upon varying the solid fraction in a broad range.

The emergence of a yield stress at sufficiently high  $\phi_{eff}$  raises the question of how a fully solid state may form. Upon flow cessation after each pre-shearing time  $\tau_1$ , we have also performed dynamic frequency sweeps. The results are reported in Fig.4. At the lowest  $\tau_1$  considered (which is however close to the point where the high-shear viscosity starts to rise dramatically) the system still behaves liquid-like as the loss modulus  $G''$  is always slightly larger than the elastic modulus  $G'$ . Upon increasing  $\tau_1$  and hence  $\phi_{eff}$ ,  $G'$  takes over with respect to  $G''$  and the ratio  $G'/G''$  becomes larger with  $\tau_1$ , while remaining mostly constant with the frequency. This is a behavior typically observed in colloidal gels [15, 28, 29] and suggests that, for the longest  $\tau_1$ , upon flow cessation the clusters are not only densely packed but can also connect into a spanning, stress-bearing structure [30]. During the shearing, in fact, the aggregates are maintained in a fluid state by the imposed high shear rate, whereas upon cessation of flow the system is subjected to a rapidly decreasing stress until a quiescent state is reached. Hence inter-aggregates connections can gradually form and become permanent as the zero stress is reached: provided that  $\phi_{eff}$  is high enough, a cohesive solid random packing of aggregates will form. To test this picture, we have calculated the elastic modulus of this disordered solid using the approach derived in [30], giving a quantitative estimate of the contribution to elasticity of inter-aggregates connections for an amorphous close-packed assembly of

aggregates of cohesive particles:

$$G' = (2/5\pi)\tilde{\kappa}\phi_{eff}\tilde{z}R_g^{-1} \quad (1)$$

where  $\tilde{z}$  is the aggregate average coordination number,  $R_g$  is their linear size and  $\tilde{\kappa}$  is the stiffness of the inter-aggregate connections formed upon flow cessation. We use this result to estimate the elastic modulus of our aggregate gel formed upon flow cessation at  $\phi_{eff} = 0.66$ , corresponding to the largest effective cluster packing fraction and the most rigid state observed, where the affine assumption underlying Eq.(1) is reasonably applicable. The irregular aggregates morphology, visible also by optical microscopy (inset of Fig.1), indicates that each connection is actually composed by many colloidal bonds (*grainy* contacts). In order to estimate the number of such bonds, we consider that for a fractal aggregate of radius  $R_g$  and fractal dimension  $d_f$ , the total number of particles is  $N_c = (R_g/a)^{d_f}$ ,  $a$  being the particle radius. Hence  $a(dN_c/dR_g) = d_f/aN_c^{(d_f-1)/d_f}$  gives the number of particles added to the outermost layer of an aggregate of radius  $R_g$ . Using  $a \simeq 60nm$ ,  $R_g \simeq 35 \pm 3\mu m$  and  $d_f \simeq 2.7$  for our system, we get the number of particles on the surface of the aggregates  $\simeq 136 \cdot 10^3$ . With an average number of 7 grainy contacts per aggregate, as for densely packed spheroidal objects [31], we can estimate that each of them involves  $n \simeq 19.4 \cdot 10^3$  particles, consistent with the value  $n \simeq 21 \cdot 10^3$  obtained measuring the contact area from optical micrographs. On this basis, we estimate  $\tilde{\kappa} = n\kappa$ , where  $\kappa = (\partial^2 U_{DLVO}/\partial r^2)_{r=r_{min}} \simeq 2 \cdot 10^{-5} N/m$ . Hence we finally obtain for the elastic modulus of our dense *gel* formed upon flow cessation,  $G' \simeq 760Pa$ , consistent with the value measured experimentally  $G' \simeq 843Pa$  at the largest  $\phi_{eff}$  (see Fig.4).

*Conclusions.* Our experiments rationalize the shear-induced solidification of a dilute, stable colloidal suspension for the first time in a fully controlled way. Large aggregates of a typical size are continuously generated under shear and behave hydrodynamically like non-Brownian hard-spheroids. Varying the shearing time leads to the same rheological response of dense non-Brownian suspensions upon varying the solid fraction. Upon flow cessation, these aggregates can eventually form *cohesive* random packings where each inter-aggregate bond involve a large number of colloidal bonds. Such solidification mechanism is thus a hybrid between colloidal gelation [32] and the packing-driven jamming [33] of non-Brownian suspensions (pastes, slurries). This scenario gives a novel insight into the complexity of the shear-induced solidification of colloidal dispersions of practical relevance.

*Acknowledgements.* This work was supported by SNSF (Grant No. 200020-126487/1). EDG is supported by the SNSF (Grant No. PP002\_126483/1).

- 
- [1] W. B. Russel, D. Saville and W. R. Schowalter, *Colloidal Dispersions*, Cambridge University Press, Cambridge (2001).
  - [2] N. A. Mody and M. R. King, *Biophys. J.* **95**, 2539 (2008); S. Rammensee *et al.*, *Proc. Natl. Acad. Sci. U.S.A.* **105**, 18 (2008); K. M. N. Oates, *et al.*, *J. Royal Soc.-Interface* **3**, 167 (2006).
  - [3] J. Vermant and M. J. Solomon, *J. Phys.: Condens. Matter* **17**, R187 (2005).
  - [4] A. J. Liu and S. R. Nagel, *Nature* **396**, 21 (1998).
  - [5] D. Xie *et al.*, *Soft Matter* **6**, 2692 (2010).
  - [6] M. Vasudevan *et al.*, *Nature Mat.* **9**, 436 (2010); I. Wunderlich, H. Hoffmann and H. Rehage, *Rheol. Acta* **26**, 532 (1987).
  - [7] A. Zacccone *et al.*, *J. Phys. Chem. B* **112**, 1976 (2008).
  - [8] P. Dimon *et al.*, *Phys. Rev. Lett.* **57**, 595 (1986).
  - [9] A. Zacccone *et al.*, *Phys. Rev. E* **80**, 051404 (2009).
  - [10] Supplementary Material: Laser light scattering analysis.
  - [11] H. Wu *et al.*, *Langmuir* **26**, 2761 (2010).
  - [12] A. Zacccone, PhD Thesis, ETH Zurich (2010).
  - [13] P. B. Warren, R. C. Ball, and A. Boelle, *Europhys. Lett.* **29**, 339 (1995).
  - [14] V. Becker *et al.*, *J. Coll. Interface Sci.* **339**, 362 (2010); M. L. Eggersdorfer *et al.*, *J. Coll. Interface Sci.* **342**, 261 (2010).
  - [15] R. G. Larson, *The Structure and Rheology of Complex Fluids* (Oxford University Press, New York, 1999) p.266.
  - [16] P. G. de Gennes, *Scaling Concepts in Polymer Physics* (Cornell Univ. Press, Ithaca NY, 1979) p.176.
  - [17] A. Zacccone *et al.*, *Phys. Rev. E* **79**, 061401 (2009).
  - [18] A. S. Moussa *et al.*, *Langmuir* **23**, 1664 (2007).
  - [19] E. Brown and H. M. Jaeger, *Phys. Rev. Lett.* **103**, 086001 (2009).
  - [20] E. Bertrand, J. Bibette, and V. Schmitt, *Phys. Rev. E* **66**, 060401 (2002).
  - [21] A. Fall *et al.*, *Phys. Rev. Lett.* **105**, 268303 (2010); A. Fall, J. Paredes, and D. Bonn, *Phys. Rev. Lett.* **105**, 225502 (2010).
  - [22] C. Bonnoit *et al.*, *Phys. Rev. Lett.* **105**, 108302 (2010); C. Bonnoit *et al.*, *J. Rheol.* **54**, 65 (2010).
  - [23] P.C.F. Moller *et al.*, *Phys. Rev. E* **77**, 041507 (2008).
  - [24] C. O. Osuji, C. Kim, and D. A. Weitz, *Phys. Rev. E* **77**, 060402 (2008)
  - [25] B. J. Maranzano and N. J. Wagner, *J. Chem. Phys.* **117**, 10291 (2002).
  - [26] E. Brown *et al.*, *Nature Mat.* **9**, 220 (2010).
  - [27] T. Divoux *et al.*, *Phys. Rev. Lett.* **104**, 208301 (2010); P. C. F. Moller, A. Fall, and D. Bonn, *EPL* **87**, 38004 (2009).
  - [28] V. Trappe and D. A. Weitz, *Phys. Rev. Lett.* **85**, 449 (2000).
  - [29] M. R. Mackley *et al.*, *Chem. Eng. Sci.* **49**, 2551 (1994).
  - [30] A. Zacccone, H. Wu, and E. Del Gado, *Phys. Rev. Lett.* **103**, 208301 (2009).
  - [31] P.M. Chaikin *et al.* *Ind. Chem. Eng. Res.* **45**, 6960 (2006).
  - [32] E. Del Gado *et al.*, *EPL* **63**, 1 (2003); A. Fierro *et al.*, *J. Stat. Mech.-Theory and Exp.* L04002 (2008); E. Del Gado and W. Kob, *Soft Matter* **6**, 1547 (2010); P.N. Segre *et al.*, *Phys. Rev. Lett.* **86**, 6042 (2001).
  - [33] M. E. Cates *et al.*, *Phys. Rev. Lett.* **81**, 1841 (1998).

## LASER LIGHT SCATTERING (LLS) ANALYSIS

After each pre-shearing, made at constant shear rate  $\dot{\gamma} = 1700s^{-1}$  for a duration  $\tau_1$ , we used LLS to investigate the structure of the suspension in terms of the structure factor which is shown in Fig.5. Immediately after sampling the rheometer, the samples were diluted to such an extent that multiple light scattering does not affect the measurement and such that the aggregates behave as noninteracting scatterers. At the shortest  $\tau_1$  considered (i.e.,  $\tau_1 < 1000s$ ), the aggregate structure factor is flat, i.e. the amount of aggregates is negligible [2]. Upon increasing  $\tau_1$ , the structure factor develops a plateau at low wave-vector  $q$ , indicative of large clusters, followed by the power-law regime of fractal objects [3]. Up to  $\tau_1 = 4893s$ , the power-law regime is followed by a flat tail which indicates that the system is still dominated by *free* primary colloidal spheres coexisting with a few very large clusters and negligible amounts of clusters of intermediate size. Confirmation of this bimodal size distribution of the aggregates comes from the analysis of the samples after filtration with a  $5\mu m$ -pore size filter which allows us to remove the large clusters from the sample. The filtered sample is then analyzed by LLS and found to be composed only by oligomers (monomers, dimers, and trimers) [4, 5]. The gyration radius of the large clusters

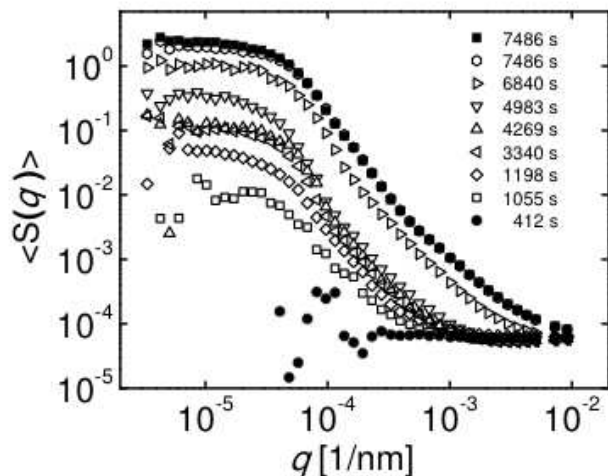


FIG. 5. (color online). The scattered intensity of the dilute system,  $I(q)$ , divided by the independently measured form factor of the latex spheres,  $P(q)$ , yields the average structure factor of the aggregates  $\langle S(q) \rangle = I(q)/P(q)$  [6], for increasing pre-shearing time  $\tau_1$  (from bottom to top).

has been estimated from the scattering curves at different shearing times through the Guinier plot and is reported in the main frame of Fig.6. The observed plateau in the cluster linear size clearly indicates that the aggregation under shear rapidly leads to a maximal cluster size  $R_g \simeq 35 \pm 3\mu m$ . The Guinier analysis in this regime is

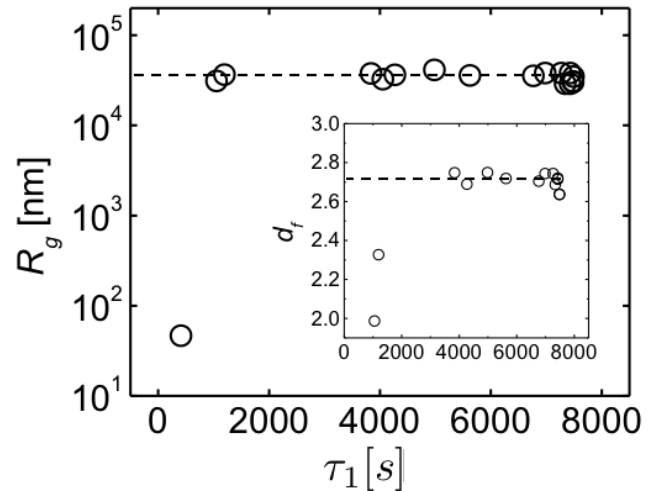


FIG. 6. (color online). Main frame: Average radius of gyration  $R_g$  of the clusters (from the Guinier plot) as a function of  $\tau_1$ . Inset (left): Average fractal dimension of the clusters  $d_f$  as a function of  $\tau_1$ .

still applicable, as the lowest scattering angle of our instrument is  $0.0145^\circ$ , i.e. well below the limit of  $0.1^\circ$  corresponding to the typical value of  $R_g$ . From the power-law regime of the scattering curves we also evaluate the fractal dimension  $d_f$  of the large clusters as a function of the shearing time (inset of Fig.6). The time evolution of  $d_f$  also rapidly reaches a plateau at  $d_f \simeq 2.7$ . Such a fairly high fractal dimension is typical of the shear-driven aggregation mechanism [6] and also results from the restructuring induced by flow stresses and breakage events [7]. Finally we have measured the fraction  $\chi(t)$  of pri-

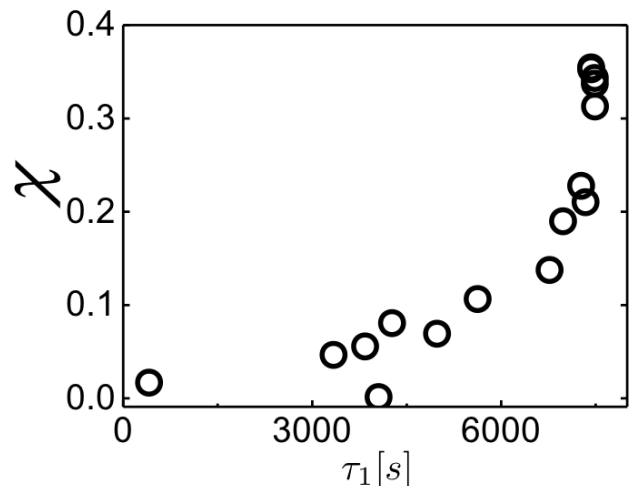


FIG. 7. (color online). Fraction  $\chi$  of primary colloidal particles converted to large aggregates at constant shear rate ( $\dot{\gamma} = 1700s^{-1}$ ) as a function of the pre-shearing time  $\tau_1$ .

mary colloidal particles converted to clusters and found

that it steeply increases with the pre-shearing time as shown in Fig.7. The fact that the size and morphology of the clusters remain constant with time indicates that under shear the system is constantly generating new clusters with approximately the same size ( $\simeq 35 \pm 5 \mu m$  of radius) and  $d_f \simeq 2.7 \pm 0.1$ . The fast increase in the number density of clusters which are fractal and porous is associated with a rapid increase of their effective packing fraction.

- 
- [1] A. Zaccone, H. Wu, D. Gentili, and M. Morbidelli, *Phys. Rev. E* 80, 051404 (2009).
  - [2] A. Zaccone et al., *J. Phys. Chem. B* 112, 1976 (2008).
  - [3] P. Dimon et al. *Phys. Rev. Lett.* 57, 595 (1986).
  - [4] H. Wu et al., *Langmuir* 26, 2761 (2010).
  - [5] A. Zaccone, PhD Thesis, ETH Zurich (2010); arXiv:1004.2237.
  - [6] P. B. Warren, R. C. Ball, and A. Boelle, *Europhys. Lett.* 29, 339 (1995).
  - [7] V. Becker et al., *J. Coll. Interface Sci.* 339, 362 (2010); M. L. Eggersdorfer, D. Kadau, H. J. Herrmann, and S. E. Pratsinis, *J. Coll. Interface Sci.* 342, 261 (2010).